

11. Local Hypercomplex Signal Representations and Applications*

Thomas Bülow and Gerald Sommer

Institute of Computer Science and Applied Mathematics,
Christian-Albrechts-University of Kiel

11.1 Introduction

The concept of the analytic signal is an important concept in one-dimensional signal theory since it makes the instantaneous amplitude and phase of a real signal directly accessible. Regrettably, there is no straightforward extension of this concept to multidimensional signals, yet. There are rather different approaches to an extension which have different drawbacks. In the first part of this chapter we will review the main approaches and introduce a new one which overcomes some of the problems of the older approaches. The new definition is easily described in the frequency domain. However, in contrast to the 1-D analytic signal we will use the quaternionic frequency domain instead of the complex Fourier domain. Based on the so defined quaternionic analytic signal [36] the instantaneous amplitude and quaternionic phase of a 2-D signal can be defined [34].

In one-dimensional signal theory it is often useful not to calculate the analytic signal but a bandpass filtered version of the analytic signal. This is done by applying so called quadrature filters. Here, we will use Gabor filters which are good approximations to quadrature filters. Corresponding to the evaluation of the quaternionic analytic signal is the application of quaternionic

* This work has been supported by German National Merit Foundation and by DFG Grants So-320-2-1 and So-320-2-2.

Gabor filters which we introduce based on the quaternionic Fourier transform. As a practical example we demonstrate the application of quaternionic Gabor filters in texture segmentation.

11.2 The Analytic Signal

The notion of the analytic signal of a real one-dimensional signal was introduced in 1946 by Gabor [88]. Before going into technical details we will give a vivid explanation of the meaning of the analytic signal. If we regard a real one-dimensional signal f as varying with time, it can be represented by the oscillating vector from the origin to $f(t)$ on the real line. Taking a snapshot of the vector at time t_0 as shown in figure 11.2 reveals no information about the amplitude or the instantaneous phase of the oscillation. I.e. it is invisible whether f is still growing to the right or already on the returning way and where the extrema of the oscillation lie. The analytic signal of f is a complex-valued signal, denoted by f_A . Thus, f_A can be visualized as a rotating vector in the complex plane. This vector has the property that its projection to the real axis is identical to the vector given by f . Moreover, if a snapshot is taken, the length of the vector, and its angle against the real axis give the instantaneous amplitude and the instantaneous phase of f , respectively. The analytic signal is constructed by adding to the real signal f a signal which is shifted by $-\pi/2$ in phase against f .

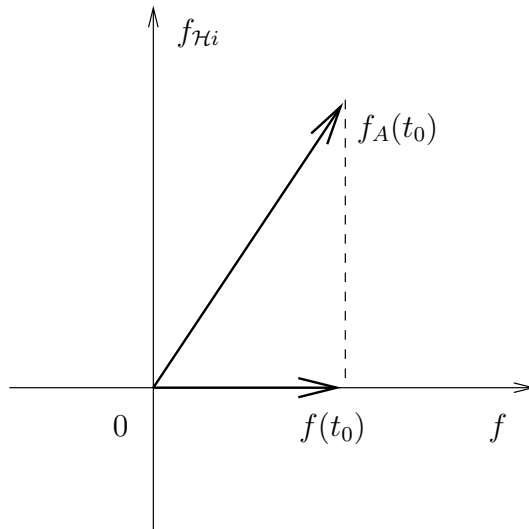


Fig. 11.1. Snapshot of the oscillating vector to f and the rotating vector to f_A at time t_0

In this section we will shortly review the analytic signal in 1-D and four approaches to the analytic signal in 2-D which have occurred in the literature [100, 101, 92, 226]. We investigate the different principles which lie at the basis of the definitions and conclude with a set of desirable properties of the 2-D analytic signal. Based on the QFT it is possible to introduce a novel definition of the analytic signal which fulfills most of the desired properties.

11.2.1 The One-Dimensional Analytic Signal

As mentioned above, the analytic signal f_A of a real one-dimensional signal f is defined as the sum of f and a $-\pi/2$ -shifted version of f as imaginary part. The shifted version of f is the Hilbert transform $f_{\mathcal{H}i}$ of f . Thus, the analytic signal can be written as $f_A = f + if_{\mathcal{H}i}$. This is the generalization of the complex notation of harmonic signals given by Euler's equation $\exp(i2\pi ux) = \cos(2\pi ux) + i \sin(2\pi ux)$.

A phase shift by $-\pi/2$ – which is expected to be done by the Hilbert transform – can be realized by taking the negative derivative of a function. E.g. we have

$$-\frac{\partial}{\partial x} \cos(2\pi ux) = 2\pi u \sin(2\pi ux),$$

which shifts the cosine-function and additionally scales the amplitude with the angular frequency $\omega = 2\pi u$. In order to avoid this extra scaling we divide each frequency component by the absolute value of the angular frequency. This procedure can easily be described in the Fourier domain: Taking the negative derivative results in multiplication by $-i2\pi u$. Dividing by $|2\pi u|$ results in the following procedure in the frequency domain:

$$F(u) \mapsto -i \frac{u}{|u|} F(u) = -i \operatorname{sign}(u) F(u),$$

which makes plausible the definition of the Hilbert transform.

The formal definitions of the Hilbert transform and of the analytic signal are as follows:

Definition 11.2.1 (Hilbert transform). *Let f be a real 1-D signal and F its Fourier transform. The Hilbert transform of f is then defined in the frequency domain by*

$$F_{\mathcal{H}i}(u) = -i \operatorname{sign}(u) F(u) \quad \text{with} \quad \operatorname{sign}(u) = \begin{cases} 1 & \text{if } u > 0 \\ 0 & \text{if } u = 0 \\ -1 & \text{if } u < 0 \end{cases}. \quad (11.1)$$

In spatial domain this reads

$$f_{\mathcal{H}i}(x) = f(x) * \frac{1}{\pi x}, \quad (11.2)$$

where $$ denotes the convolution operation.*

The convolution integral in (11.2), namely

$$f_{\mathcal{H}i}(x) = \frac{1}{\pi} \int_{\mathbb{R}} \frac{f(\xi)}{x - \xi} d\xi$$

contains a singularity at $x = \xi$. This is handled by evaluating Cauchy's principle value, i.e.

$$f_{\mathcal{H}i}(x) = \frac{1}{\pi} P \int_{\mathbb{R}} \frac{f(\xi)}{x - \xi} d\xi \quad (11.3)$$

$$= \frac{1}{\pi} \lim_{\epsilon \rightarrow 0} \left(\int_{-\infty}^{x-\epsilon} \frac{f(\xi)}{x - \xi} d\xi + \int_{x+\epsilon}^{\infty} \frac{f(\xi)}{x - \xi} d\xi \right) \quad (11.4)$$

Definition 11.2.2 (Analytic signal). Let f be a real 1-D signal and F its Fourier transform. Its analytic signal in the Fourier domain is then given by

$$\begin{aligned} F_A(u) &= F(u) + iF_{\mathcal{H}i}(u) \\ &= F(u)(1 + \text{sign}(u)). \end{aligned} \quad (11.5)$$

In the spatial domain this definition reads:

$$f_A(x) = f(x) + if_{\mathcal{H}i}(x) = f(x) * \left(\delta(x) + \frac{i}{\pi x} \right). \quad (11.6)$$

Thus, the analytic signal of f is constructed by taking the Fourier transform F of f , suppressing the negative frequencies and multiplying the positive frequencies by two. Note that, applying this procedure, we do not lose any information about f because of the Hermite symmetry of the spectrum of a real function.

The analytic signal enables us to define the notions of the instantaneous amplitude and the instantaneous phase of a signal [92].

Definition 11.2.3 (Instantaneous amplitude and phase). Let f be a real 1-D signal and f_A its analytic signal. The instantaneous amplitude and phase of f are then defined by

$$\text{instantaneous amplitude of } f(x) = |f_A(x)| \quad (11.7)$$

$$\text{instantaneous phase of } f(x) = \text{atan2}(\mathcal{I}f_A(x), \mathcal{R}f_A(x)). \quad (11.8)$$

For later use we introduce the notion of a Hilbert pair.

Definition 11.2.4 (Hilbert pair). Two real one-dimensional functions f and g are called a Hilbert pair if one is the Hilbert transform of the other, i.e.

$$f_{\mathcal{H}i} = g \quad \text{or} \quad g_{\mathcal{H}i} = f.$$

If $f_{\mathcal{H}i} = g$ it follows that $g_{\mathcal{H}i} = -f$.

We illustrate the above definitions by a simple example: The analytic signal of $f(x) = a \cos(\omega x)$ which is $a \cos_A(\omega x) = a \cos(\omega x) + ia \sin(\omega x) = a \exp(i\omega x)$. The instantaneous amplitude of f is given by $|f_A(x)| = a$ while the instantaneous phase is $\text{atan2}(\mathcal{I}f_A(x), \mathcal{R}f_A(x)) = \omega x$. Thus, the instantaneous amplitude and phase of the cosine-function are exactly equal to the expected values a and ωx , respectively. Furthermore, \cos and \sin constitute a *Hilbert pair*. Figure 11.2 shows another example of an oscillating signal together with its instantaneous amplitude and its instantaneous phase.

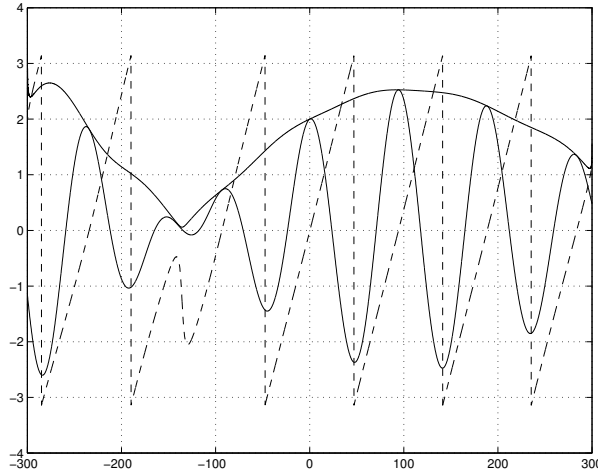


Fig. 11.2. An oscillating signal, its instantaneous amplitude (signal envelope) and its instantaneous phase (dashed)

However, the close relation of the instantaneous amplitude and phase to the local structure of the signal gets lost if the signal has no well defined angular frequency. Most of the time it is sufficient to require the signal to be of narrow bandwidth ([92], p. 171).

For this reason later (in section 11.3.1) Gabor filters will be introduced which establish a relation between the local structure and the local phase of a broader class of signals.

11.2.2 Complex Approaches to the Two-Dimensional Analytic Signal

The construction of the analytic signal is of interest not only in one-dimensional signal processing but in image processing and multidimensional signal processing as well. So far, however, we have merely presented a definition of the one-dimensional analytic signal. Thus, an extension to higher

dimensions is needed. There have appeared different approaches to a 2-D analytic signal in the literature. All of these approaches use a combination of the original signal and its Hilbert transform. In this section we will present and discuss these approaches. A novel approach which is based on the quaternionic Fourier transform (see chap. 8, Def. 8.3.4) is introduced in section 11.2.3.

In order to evaluate the different approaches to the analytic signal to 2-D we need some guidelines. As such a guideline we give a list of the main properties of the analytic signal in 1-D. Any new definition will be measured according to the degree to which it extends these properties to higher dimensions.

Table 11.1. Four properties of the analytic signal

1.	The spectrum of an analytic signal is right-sided ($F_A(u) = 0$ for $u < 0$).
2.	Hilbert pairs are orthogonal.
3.	The real part of the analytic signal f_A is equal to the original signal f .
4.	The analytic signal is compatible with the associated harmonic transform (in case of the 1-D analytic signal with the Fourier transform.)

We will explain the forth point. The analytic signal is called compatible with the associated harmonic transform with transformation kernel K if $\mathcal{R}K$ and $\mathcal{I}K$ are a Hilbert pair. In case of the one-dimensional Fourier transform this property is fulfilled, since the real part of the Fourier kernel, i.e. $\mathcal{R}(\exp(-i2\pi ux)) = \cos(-2\pi ux)$ is the Hilbert transform of $\sin(-2\pi ux)$, as was shown above.

The first definition is based on the 2-D Hilbert transform [226]:

Definition 11.2.5 (Total 2-D Hilbert transform). *Let f be a real two-dimensional signal. Its Hilbert transform is given by*

$$f_{\mathcal{H}i}(\mathbf{x}) = f(\mathbf{x}) * \left(\frac{1}{\pi^2 xy} \right), \quad (11.9)$$

where $*$ denotes the 2-D convolution. In the frequency domain this reads

$$F_{\mathcal{H}i}(\mathbf{u}) = -F(\mathbf{u}) \operatorname{sign}(u) \operatorname{sign}(v).$$

Sometimes $f_{\mathcal{H}i}$ is called the total Hilbert transform of f [101].

For later use, we define also the partial Hilbert transforms of a 2-D signal.

Definition 11.2.6 (Partial Hilbert transform).

Let f be a real two-dimensional signal. Its partial Hilbert transforms in x - and y -direction are given by

$$f_{\mathcal{H}i_1}(\mathbf{x}) = f(\mathbf{x}) * \left(\frac{\delta(y)}{\pi x} \right), \quad \text{and} \quad (11.10)$$

$$f_{\mathcal{H}i_2}(\mathbf{x}) = f(\mathbf{x}) * \left(\frac{\delta(x)}{\pi y} \right), \quad (11.11)$$

respectively. In the frequency domain this reads

$$F_{\mathcal{H}i_1}(\mathbf{u}) = -iF(\mathbf{u})\text{sign}(u) \quad \text{and} \quad F_{\mathcal{H}i_2}(\mathbf{u}) = -iF(\mathbf{u})\text{sign}(v).$$

The partial Hilbert transform of a 2-D signal can of course be defined with respect to any orientation.

In analogy to 1-D an extension of the analytic signal can be defined as follows:

Definition 11.2.7 (Total analytic signal). The analytic signal of a real 2-D signal f is defined as

$$f_A(\mathbf{x}) = f(\mathbf{x}) * \left(\delta^2(\mathbf{x}) + \frac{i}{\pi^2 xy} \right) \quad (11.12)$$

$$= f(\mathbf{x}) + if_{\mathcal{H}i}(\mathbf{x}), \quad (11.13)$$

where $f_{\mathcal{H}i}$ is given by (11.9). In the frequency domain this definition reads

$$F_A(\mathbf{u}) = F(\mathbf{u})(1 - i\text{sign}(u)\text{sign}(v)).$$

The spectrum of f_A according to definition 11.2.7 is shown in figure 11.3. It does not vanish anywhere in the frequency domain. Hence, there is no analogy to the causality property of an analytic signal's spectrum in 1-D. Secondly, Hilbert pairs according to this definition are only orthogonal if the functions are separable [101]. Furthermore, the above definition of the analytic signal is not compatible with the two-dimensional Fourier transform, since $\sin(2\pi\mathbf{u}\mathbf{x})$ is not the total Hilbert transform of $\cos(2\pi\mathbf{u}\mathbf{x})$. Thus, the properties 1, 2 and 4 from table 11.1 are not satisfied by this definition. A

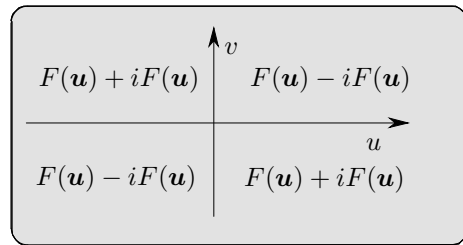


Fig. 11.3. The spectrum of the analytic signal according to definition 11.2.7

common approach to overcome this fact can be found e.g. by Granlund [92]. This definition starts with the construction in the frequency domain. While in 1-D the analytic signal is achieved by suppressing the negative frequency components, in 2-D one half-plane of the frequency domain is set to zero in order to fulfill the causality constraint (property no. 1 in table 11.1). It is not immediately clear how negative frequencies can be defined in 2-D. However, it is possible to introduce a direction of reference defined by the unit vector $\hat{\mathbf{e}} = (\cos(\theta), \sin(\theta))$. A frequency \mathbf{u} with $\hat{\mathbf{e}} \cdot \mathbf{u} > 0$ is called positive while a frequency with $\hat{\mathbf{e}} \cdot \mathbf{u} < 0$ is called negative. The 2-D analytic signal can then be defined in the frequency domain.

Definition 11.2.8 (Partial analytic signal). *Let f be a real 2-D signal and F its Fourier transform. The Fourier transform of the analytic signal is defined by:*

$$F_A(\mathbf{u}) = \begin{cases} 2F(\mathbf{u}) & \text{if } \mathbf{u} \cdot \hat{\mathbf{e}} > 0 \\ F(\mathbf{u}) & \text{if } \mathbf{u} \cdot \hat{\mathbf{e}} = 0 \\ 0 & \text{if } \mathbf{u} \cdot \hat{\mathbf{e}} < 0 \end{cases} = F(\mathbf{u})(1 + \text{sign}(\mathbf{u} \cdot \hat{\mathbf{e}})). \quad (11.14)$$

In the spatial domain (11.14) reads

$$f_A(\mathbf{x}) = f(\mathbf{x}) * \left(\delta(\mathbf{x} \cdot \hat{\mathbf{e}}) + \frac{i}{\pi \mathbf{x} \cdot \hat{\mathbf{e}}} \right) \delta(\mathbf{x} \cdot \hat{\mathbf{e}}_{\perp}). \quad (11.15)$$

The vector $\hat{\mathbf{e}}_{\perp}$ is a unit vector which is orthogonal to $\hat{\mathbf{e}}$: $\hat{\mathbf{e}} \cdot \hat{\mathbf{e}}_{\perp} = 0$.

Please note the similarity of this definition with the one-dimensional definition (11.5). For $\hat{\mathbf{e}}^{\top} = (1, 0)$ (11.15) takes the form

$$f_A(\mathbf{x}) = f(\mathbf{x}) * \left(\delta(x) + \frac{i}{\pi x} \right) \delta(y) \quad (11.16)$$

$$= f(\mathbf{x}) + if_{\mathcal{H}i_1}. \quad (11.17)$$

Thus, the reason for the name *partial analytic signal* lies in the fact that it is the sum of the original signal and the partial Hilbert transform as imaginary part. The partial analytic signal with respect to the two coordinate axes has been used by Venkatesh et al. [242, 241] for the detection of image features. They define the energy maxima of the partial analytic signal as image features.

According to this definition the analytic signal is calculated line-wise along the direction of reference. The lines are processed independently. Hence, definition 11.2.8 is intrinsically 1-D, such that it is no satisfactory extension of the analytic signal to 2-D. Its application is reasonable only for simple signals, i.e. signals which vary only along one orientation [92]. The orientation $\hat{\mathbf{e}}$ can then be chosen according to the direction of variation of the image.

If negative frequencies are defined in the way indicated above, we can say that property 1 of table 11.1 is fulfilled. Properties 2 and 3 are valid as well.

This follows from the fact that merely the 1-D analytic signal is evaluated line-wise, which leads to a trivial extension of these properties. Even property 4 is "almost" valid: $\sin(ux+vy)$ is the partial Hermite transform (i.e. with respect to the x direction) of $\cos(ux+vy)$ for all frequencies \mathbf{u} with $u \neq 0$. However, the main drawback of definition 11.2.8 is the intrinsic one-dimensionality of the definition and the non-uniqueness with regard to the orientation of reference $\hat{\mathbf{e}}$.

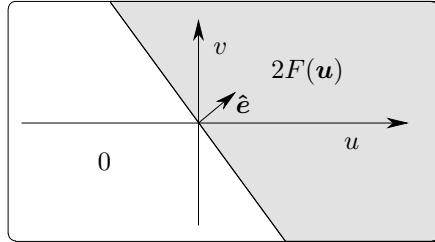


Fig. 11.4. The spectrum of the analytic signal according to definition 11.2.8

The both definitions presented so far seem to establish the following dilemma: Either an intrinsically two-dimensional definition of the analytic signal based on the total Hilbert transform can be introduced, which does not extend the main properties of the 1-D analytic signal, or these properties are extended by an intrinsically one-dimensional definition based on the partial Hilbert transform.

An alternative to these approaches was recently introduced by Hahn [100, 101]. Hahn avoids the term "analytic signal" and uses Gabor's original term "complex signal" instead.

Definition 11.2.9. Let f be a real, two-dimensional function and F its Fourier transform. The 2-D complex signal (according to Hahn [101]) is defined in the frequency domain by

$$F_A(\mathbf{u}) = (1 + \text{sign}(u))(1 + \text{sign}(v))F(\mathbf{u}).$$

In the spatial domain this reads

$$f_A(\mathbf{x}) = f(\mathbf{x}) * \left(\delta(x) + \frac{i}{\pi x} \right) \left(\delta(y) + \frac{i}{\pi y} \right) \quad (11.18)$$

$$= f(\mathbf{x}) - f_{\mathcal{H}_i}(\mathbf{x}) + i(f_{\mathcal{H}_{i_1}}(\mathbf{x}) + f_{\mathcal{H}_{i_2}}(\mathbf{x})), \quad (11.19)$$

where $f_{\mathcal{H}_i}$ is the total Hilbert transform, and $f_{\mathcal{H}_{i_1}}$ and $f_{\mathcal{H}_{i_2}}$ are the partial Hilbert transforms.

The meaning of definition 11.2.9 becomes clear in the frequency domain: Only the frequency components with $u > 0$ and $v > 0$ are kept, while the components in the three other quadrants are suppressed (see figure 11.5):

$$F_A(\mathbf{u}) = (1 + \text{sign}(u))(1 + \text{sign}(v))F(\mathbf{u}).$$

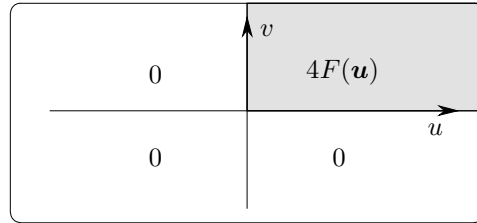


Fig. 11.5. The spectrum of the analytic signal according to Hahn [100] (definition 11.2.9)

Thus, the problem of defining positive frequencies is solved in another way than in definition 11.2.8.

A main problem of definition 11.2.9 is the fact that the original signal is not reconstructible from the analytic signal, since due to the Hermite symmetry only one half-plane of the frequency domain of a real signal is redundant. For this reason Hahn proposes to calculate not only the analytic signal with the spectrum in the upper right quadrant but also another analytic signal with its spectrum in the upper left quadrant. It can be shown that these two analytic signals together contain all the information of the original signal [101]. When necessary we distinguish the two analytic or complex signals by referring to them as definition 11.2.9a and 11.2.9b, respectively.

Thus, the complete analytic signal according to definition 11.2.9 consists of two complex signals, i.e. two real parts and two imaginary parts or, in polar representation, of two amplitude- and two phase-components which makes the interpretation, especially of the amplitude, difficult. Furthermore, it would be more elegant to express the analytic signal with only one function instead of two. Definition 11.2.9 fulfills properties 1 and 2 from table 11.1. The very important property that the signal should be reconstructible from its analytic signal is only fulfilled if two different complex signals are calculated using two neighbored quadrants of the frequency domain. Hahn [101] mentions that his definition of the 2-D analytic signal is compatible with the 2-D Fourier transform for the following reason: The 2-D Fourier kernel can be written in the form

$$\exp(i2\pi\mathbf{u}\mathbf{x}) = \cos(2\pi ux) \cos(2\pi vy) - \sin(2\pi ux) \sin(2\pi vy) \quad (11.20)$$

$$+ i(\cos(2\pi ux) \sin(2\pi vy) + \sin(2\pi ux) \cos(2\pi vy)) \quad (11.21)$$

where for convenience we have omitted the minus sign in the exponential. According to definition 11.2.9 this is exactly the complex signal of $f(\mathbf{x}) = \cos(2\pi ux) \cos(2\pi vy)$. However, this fulfills only a weak kind of compatibility and not the one defined by us above. This would require that the analytic signal of $\mathcal{R} \exp(i2\pi\mathbf{u}\mathbf{x})$ would equal $\exp(i2\pi\mathbf{u}\mathbf{x})$.

The remaining problems can be summarized as follows. The original signal cannot be recovered from Hahn's analytic signal. This restriction can only be overcome by introducing two complex signals for each real signal, which is not a satisfactory solution. Furthermore, Hahn's analytic signal is not compatible with the 2-D Fourier transform in the strong sense.

Apart from these disadvantages, it is clear from the above analysis, that, among the definitions introduced so far, Hahn's definition is closest to a satisfactory 2-D extension of the analytic signal. In the following section we will show how Hahn's frequency domain construction can be applied to the construction of a quaternionic analytic signal, which overcomes the remaining problems.

11.2.3 The 2-D Quaternionic Analytic Signal

Hahn's approach to the analytic signal faces the problem that a two-dimensional complex hermitian signal can not be recovered from one quadrant of its domain. For this reason Hahn introduced two complex signals to each real two-dimensional signal. We will show how this problem is solved using the QFT.

Since the QFT of a real signal is quaternionic hermitian (see chapter 8, theorem 8.4.8) we do not lose any information about the signal in this case. This fact is visualized in figure 11.6.

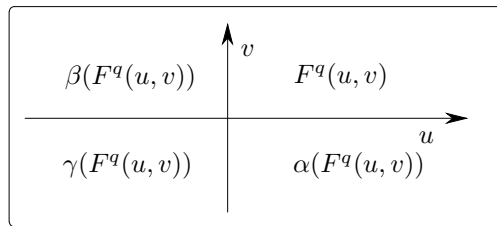


Fig. 11.6. The quaternionic spectrum of a real signal can be reconstructed from only one quadrant

Thus, we define the quaternionic analytic signal in the frequency domain as in definition 11.2.9, with the only difference that we use the quaternionic frequency domain defined by the QFT instead of the complex frequency domain.

Definition 11.2.10 (Quaternionic analytic signal). *Let f be a real two-dimensional signal and F^q its QFT. In the quaternionic frequency domain we define the quaternionic analytic signal of a real signal as*

$$F_A^q(\mathbf{u}) = (1 + \text{sign}(u))(1 + \text{sign}(v))F^q(\mathbf{u}),$$

where $\mathbf{x} = (x, y)$ and $\mathbf{u} = (u, v)$. Definition 11.2.10 can be expressed in the spatial domain as follows:

$$f_A^q(\mathbf{x}) = f(\mathbf{x}) + \mathbf{n} \cdot \mathbf{f}_{\mathcal{H}i}(\mathbf{x}), \quad (11.22)$$

where $\mathbf{n} = (i, j, k)^\top$ and $\mathbf{f}_{\mathcal{H}i}$ is a vector which consists of the total and the partial Hilbert transforms of f according to definitions 11.2.5 and 11.2.6:

$$\mathbf{f}_{\mathcal{H}i}(\mathbf{x}) = \begin{pmatrix} f_{\mathcal{H}i_1}(\mathbf{x}) \\ f_{\mathcal{H}i_2}(\mathbf{x}) \\ f_{\mathcal{H}i}(\mathbf{x}) \end{pmatrix}. \quad (11.23)$$

Note that, formally, (11.22) resembles the definition of the one-dimensional analytic signal (11.6). Since the quaternionic analytic signal consists of four components we replace the notion of a Hilbert pair (definition 11.2.4) by the notion of a *Hilbert quadruple*.

Definition 11.2.11 (Hilbert quadruple). *Four real two-dimensional functions f_i , $i \in \{1, \dots, 4\}$ are called a Hilbert quadruple if*

$$\mathcal{I}(f_k)_A^q = f_l \quad (11.24)$$

$$\mathcal{J}(f_k)_A^q = f_m \quad (11.25)$$

$$\mathcal{K}(f_k)_A^q = f_n \quad (11.26)$$

for some permutation of pairwise different $k, l, m, n \in \{1, \dots, 4\}$.

Theorem 11.2.1. *The four components of the QFT-kernel build a Hilbert quadruple.*

Proof. Since the quaternionic analytic signal of $f(\mathbf{x}) = \cos(\omega_x x) \cos(\omega_y y)$ is given by $f_A^q(\mathbf{x}) = \exp(i\omega_x x) \exp(j\omega_y y)$, which is the QFT-kernel, we have

$$\mathcal{I}(\mathcal{R} \exp(i\omega_x x) \exp(j\omega_y y))_A^q = \mathcal{I} \exp(i\omega_x x) \exp(j\omega_y y) \quad (11.27)$$

$$\mathcal{J}(\mathcal{R} \exp(i\omega_x x) \exp(j\omega_y y))_A^q = \mathcal{J} \exp(i\omega_x x) \exp(j\omega_y y) \quad (11.28)$$

$$\mathcal{K}(\mathcal{R} \exp(i\omega_x x) \exp(j\omega_y y))_A^q = \mathcal{K} \exp(i\omega_x x) \exp(j\omega_y y). \quad (11.29)$$

which concludes the proof. \square

11.2.4 Instantaneous Amplitude

One main feature of the analytic signal is that it makes accessible instantaneous phase and amplitude information directly. In the following we define the instantaneous amplitude of real 2-D signal as the absolute value of its analytic signal. Clearly, the different definitions of the analytic signal given in the last section result in different definitions of the instantaneous amplitude of a signal. We summarize these definitions in table 11.2. Figure 11.7 shows

analytic signal	instantaneous amplitude
Def. 11.2.7	$\sqrt{f^2(\mathbf{x}) + f_{\mathcal{H}i}^2(\mathbf{x})}$
Def. 11.2.8	$\sqrt{f^2(\mathbf{x}) + f_{\mathcal{H}i_1}^2(\mathbf{x})}$
Def. 11.2.9	$\sqrt{[f(\mathbf{x}) - f_{\mathcal{H}i}(\mathbf{x})]^2 + [f_{\mathcal{H}i_1}(\mathbf{x}) + f_{\mathcal{H}i_2}(\mathbf{x})]^2}$
Def. 11.2.10	$\sqrt{f^2(\mathbf{x}) + f_{\mathcal{H}i_1}^2(\mathbf{x}) + f_{\mathcal{H}i_2}^2(\mathbf{x}) + f_{\mathcal{H}i}^2(\mathbf{x})}$

Table 11.2. The tabular shows the different possible definitions of the instantaneous magnitude in 2-D. On the right hand side the instantaneous amplitude of the 2-D signal f is given according to the definition of the analytic signal indicated on the left hand side

an image of D. Hilbert and the instantaneous amplitude of this image. The instantaneous amplitude is expected to take high values wherever the image has considerable contrast. From this point of view only the instantaneous amplitude constructed via the partial analytic signal and the quaternionic analytic signal yield acceptable results. However, at positions where the local structure is intrinsically 2-D the quaternionic analytic signal yields better results.

11.2.5 The n -Dimensional Analytic Signal

All approaches to the 2-D analytic signal can easily be extended to n -dimensional signals. We merely give the definitions here and forego a detailed discussion, since the main properties of and differences between the different approaches remain the same in n -D as in 2-D.

Definition 11.2.12 (Total analytic signal). *The analytic signal of a real n -D signal f is defined as*

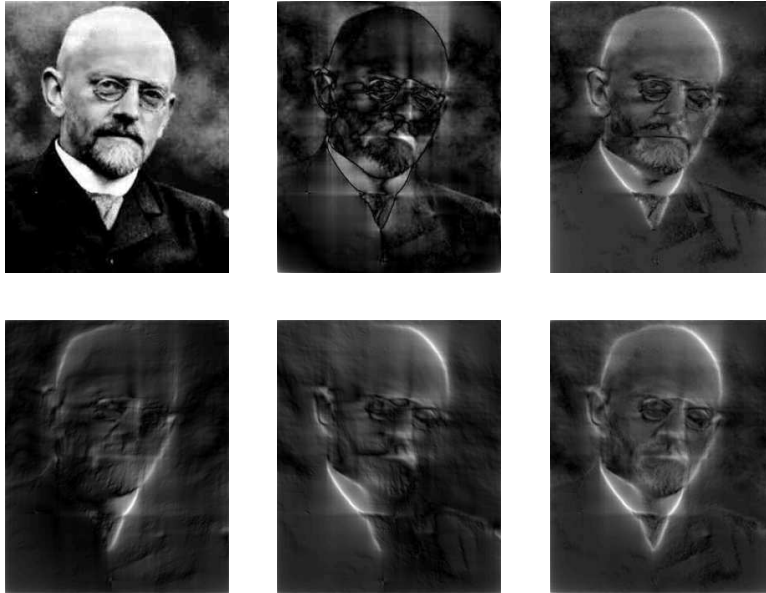


Fig. 11.7. An image of Hilbert and its instantaneous amplitude according to the different definitions of the 2-D analytic signal given in section 11.2.3. From top left to bottom right: The original image, the instantaneous amplitude (IA) according to the total analytic signal, the partial analytic signal (with respect to the x -direction), the definition of Hahn (maintaining the upper right quadrant and the upper left quadrant, respectively), and the IA with respect to the quaternionic analytic signal

$$f_A(\mathbf{x}) = f(\mathbf{x}) * \left(\delta^n(\mathbf{x}) + \frac{i}{\pi^n \prod_{j=1}^n x_j} \right) \quad (11.30)$$

$$=: f(\mathbf{x}) + i f_{\mathcal{H}_i}(\mathbf{x}), \quad (11.31)$$

where $f_{\mathcal{H}_i}$ is the n -D total Hilbert transform of f . In the frequency domain this definition reads

$$F_A(\mathbf{u}) = F(\mathbf{u}) \left(1 - i \prod_{j=1}^n \text{sign}(u_j) \right).$$

Definition 11.2.13 (Partial analytic signal). Let f be a real n -D signal and F its Fourier transform. The Fourier transform of the analytic signal with respect to some n -D unit vector $\hat{\mathbf{e}}$ is defined by:

$$F_A(\mathbf{u}) = \begin{cases} 2F(\mathbf{u}) & \text{if } \mathbf{u} \cdot \hat{\mathbf{e}} > 0 \\ F(\mathbf{u}) & \text{if } \mathbf{u} \cdot \hat{\mathbf{e}} = 0 \\ 0 & \text{if } \mathbf{u} \cdot \hat{\mathbf{e}} < 0 \end{cases} = F(\mathbf{u}) (1 + \text{sign}(\mathbf{u} \cdot \hat{\mathbf{e}})). \quad (11.32)$$

Definition 11.2.14. Let f be a real, n -dimensional function and F its Fourier transform. The n -D complex signal (according to Hahn [101]) is defined in the frequency domain by

$$F_A(\mathbf{u}) = \prod_{j=1}^n (1 + \text{sign}(u_j)) F(\mathbf{u}).$$

In the spatial domain this reads

$$f_A(\mathbf{x}) = f(\mathbf{x}) * \prod_{j=1}^n \left(\delta(x_j) + \frac{i}{\pi x_j} \right). \quad (11.33)$$

Finally we define the n -dimensional version of the quaternionic analytic signal, namely the Clifford analytic signal.

Definition 11.2.15 (Clifford analytic signal).

Let f be a real, n -dimensional function and F^c its Clifford Fourier transform. The n -D Clifford analytic signal is defined in the frequency domain by

$$F_A^c(\mathbf{u}) = \prod_{j=1}^n (1 + \text{sign}(u_j)) F^c(\mathbf{u}).$$

In the spatial domain this reads

$$f_A^c(\mathbf{x}) = f(\mathbf{x}) * \prod_{j=1}^n \left(\delta(x_j) + \frac{e_j}{\pi x_j} \right). \quad (11.34)$$

11.3 Local Phase in Image Processing

We have shown how the instantaneous phase can be evaluated using the analytic signal. However, the instantaneous phase loses its direct relation to the local signal structure, when the signal is not of narrow bandwidth [92]. In order to overcome this restriction, bandpass-filters with a one-sided transfer function can be applied to a signal. According to the definition of the 1-D analytic signal the impulse responses of these filters, and the filter responses to any real signal as well, are analytic signals. Filters of this kind are called *quadrature filters*. The angular phase of the quadrature filter response to a real signal is called the *local phase*. In the following we will introduce complex Gabor filters as approximations to quadrature filters. Using these filters we will define the local complex phase of an n -D signal. Since the local complex phase is an intrinsically 1-D concept it is a reasonable concept merely for simple or locally intrinsically 1-D signals. In section 11.3.2 we introduce quaternionic Gabor filters based on the quaternionic Fourier transform. Using these filters the concept of local phase of 2-D signals is extended.

11.3.1 Local Complex Phase

Complex Gabor filters are defined as linear shift-invariant filters with the Gaussian windowed basis functions of the Fourier transform as their basis functions.

Definition 11.3.1 (1-D Complex Gabor filter). *A one-dimensional complex Gabor filter is a linear shift-invariant filter with the impulse response*

$$h(x; N, u_0, \sigma) = g(x; N, \sigma) \exp(i2\pi u_0 x), \quad (11.35)$$

where $g(x; N, \sigma)$ is the Gauss function

$$g(x; N, \sigma) = N \exp\left(-\frac{x^2}{2\sigma^2}\right).$$

The Gabor filters have as parameters the normalization constant N , the *center frequency* u_0 and the variance σ of the Gauss function. However, most of the time we will not write down these arguments explicitly. Where no confusion is possible we use the notation $h(x)$ and $g(x)$ for the Gabor filter and the Gaussian function at position x , respectively.

We will use the normalization $N = (\sqrt{2\pi\sigma^2})^{-1}$ such that $\int_{\mathbb{R}} g(x) dx = 1$ in the following. Analogously the definition of 2-D complex Gabor filters is based on the 2-D Fourier transform:

Definition 11.3.2 (2-D Complex Gabor filter). *A two-dimensional complex Gabor filter is a linear shift-invariant filter with the impulse response*

$$h(\mathbf{x}; \mathbf{u}_0, \sigma, \epsilon, \phi) = g(x', y') \exp(2\pi i(u_0 x + v_0 y)) \quad (11.36)$$

with

$$g(x, y) = N \exp\left(-\frac{x^2 + (\epsilon y)^2}{\sigma^2}\right)$$

where ϵ is the aspect ratio. The coordinates (x', y') are derived from (x, y) by a rotation about the origin through the angle ϕ :

$$\begin{pmatrix} x' \\ y' \end{pmatrix} = \begin{pmatrix} \cos \phi & \sin \phi \\ -\sin \phi & \cos \phi \end{pmatrix} \begin{pmatrix} x \\ y \end{pmatrix}. \quad (11.37)$$

Again, we will choose the normalization such that $\int_{\mathbb{R}} g(x, y) dx dy = 1$, i.e. $N = \frac{\epsilon}{2\pi\sigma^2}$. In frequency domain the 1-D Gabor filters take the following form:

$$h(x; u_0, \sigma) \circ\bullet H(u; u_0, \sigma) = \exp(-2\pi^2\sigma^2(u - u_0)^2).$$

The transfer function of a 2-D Gabor filter is given by

$$h(\mathbf{x}; \mathbf{u}_0, \sigma, \epsilon, \phi) \circ\bullet H(\mathbf{u}; \mathbf{u}_0, \sigma, \epsilon, \phi) = \exp(-2\pi^2\sigma^2[|\mathbf{u}' - \mathbf{u}'_0|^2/\epsilon]).$$

Thus, Gabor filters are bandpass filters. The radial center frequency of the 2-D Gabor filter is given by $F = \sqrt{u_0^2 + v_0^2}$ and its orientation is $\theta = \text{atan}(v_0/u_0)$. In most cases it is convenient to choose $\theta = \phi$ such that the orientation of the complex sine gratings is identical with the orientation of one of the principle axes of the Gauss function. Figure 11.8 shows the transfer function of a one-dimensional complex Gabor filter. Figure 11.8 shows that

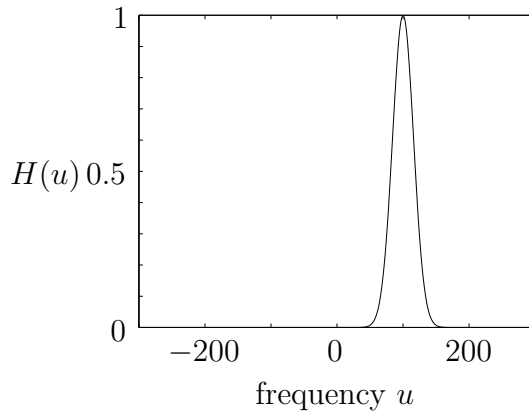


Fig. 11.8. The transfer function of a one-dimensional Gabor filter with $u_0 = 100$ and $\sigma = 0.01$

the main amount of energy of the Gabor filter is centered around the center frequency u_0 in the positive half of the frequency domain. However, the energy in the negative half is not equal to zero. Because of this property, the filter response of the Gabor filter to a real signal is only an approximation

to an analytic signal (which is only one-sided in the frequency domain). The error of this approximation decreases with increasing u and with increasing σ .

The *local phase* of a signal is defined as the angular phase of its complex Gabor filter response. The relation to the local structure of the signal becomes clear in the following way. At a signal position with locally even symmetry only the even part of the Gabor filter, which is real-valued matches. The angular phase of a real number is either 0 for a positive number or π for a negative one. Thus, if the even filter component matches the signal positive, the local phase is 0, if it matches negative, the local phase is π . A similar reflection clarifies the case of a locally odd structure. In this case only the odd, and thus imaginary, filter component matches the signal. Since the angular phase of a pure imaginary number is $\pi/2$ for a positive imaginary part and $-\pi/2$ otherwise, these values represent odd local structures. Figure 11.9 sketches the relation between structure and phase: the orientation in the circle indicates the value of the local phase. At the values 0, $\pi/2$, π and $-\pi/2$ the related structure is shown. An important feature of the **local phase** is

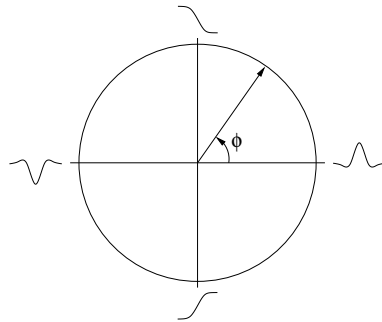


Fig. 11.9. The relation between local signal structure and local phase (See [92].)

that it is **independent of the signal energy**. This makes the local phase very robust against changing lighting conditions.

It should be mentioned here that the value of the local phase at a certain signal position depends on the chosen filter parameters. I.e. Gabor filters will only detect features at the scale to which they are tuned.

11.3.2 Quaternionic Gabor Filters

In analogy to the complex Gabor filters we introduce quaternionic Gabor filters.

Definition 11.3.3 (Quaternionic Gabor filter). *The impulse response of a quaternionic Gabor filter is a Gaussian windowed basis function of the QFT:*

$$h^q(\mathbf{x}; \mathbf{u}_0, \sigma, \epsilon) = g(\mathbf{x}; \sigma, \epsilon) \exp(i2\pi u_0 x) \exp(j2\pi v_0 y). \quad (11.38)$$

Note that we do not use rotated Gaussian windows here.

It follows from the modulation theorem of the Fourier transform that complex Gabor filters are shifted Gaussians in the frequency domain. In section 8.4.2 of chapter 8 we showed that there exists a modulation theorem for the QFT as well. Consequently, quaternionic Gabor filters are shifted Gaussian functions in the quaternionic frequency domain. Quaternionic Gabor filters thus belong to the "world" of the QFT rather than to the "complex Fourier world". The QFT of a quaternionic Gabor filter is given by

$$h^q(\mathbf{x}; \mathbf{u}_0, \sigma, \epsilon) \overset{\mathbb{H}}{\circlearrowleft} H^q(\mathbf{u}; \mathbf{u}_0, \sigma, \epsilon) = \exp(-2\pi^2 \sigma^2 [|\mathbf{u} - \mathbf{u}_0|^2 / \epsilon^2])$$

Thus, for positive frequencies u_0 and v_0 the main amount of the Gabor filter's energy lies in the upper right quadrant. Therefore, convolving a real signal with a quaternionic Gabor filter yields an approximation to a quaternionic analytic signal.

A typical quaternionic Gabor filter is shown in figure 11.10.

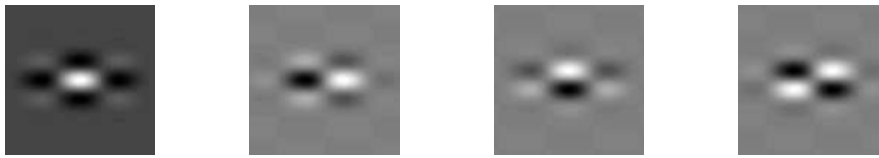


Fig. 11.10. A quaternionic Gabor filter with parameters $\sigma_1 = 20$, $\sigma_2 = 10$, $2\pi u_0 \sigma_1 = 2\pi v_0 \sigma_2 = 2$. The size of the filter mask is 100×100

11.3.3 Local Quaternionic Phase

We now define the local quaternionic phase of a real two-dimensional signal as the angular phase of the filter response to a quaternionic Gabor filter. The angular phase is evaluated according to the rules given in table 8.1. If k^q is the quaternionic Gabor filter response of some image f the local quaternionic phase $(\phi(\mathbf{x}), \theta(\mathbf{x}), \psi(\mathbf{x}))$ is defined by

$$k^q(\mathbf{x}) = |k^q(\mathbf{x})| e^{i\phi(\mathbf{x})} e^{k\psi(\mathbf{x})} e^{j\theta(\mathbf{x})}$$

according to def. 8.3.1 given in chapter 8.

In 1-D we can make the statement: **The local phase estimates and spatial position are equivariant** [92]. I.e. generally the local phase of a signal varies monotonically up to 2π -wrap-arounds. There are only singular

points with low or zero signal energy where this equivariance cannot be found anymore. A simple example is the cosine function $\cos(x)$. If we apply a well tuned Gabor filter for estimating the local phase ϕ of this function, we find that it is almost equal to the spatial position: $\phi(x) \approx x$ for $x \in [-\pi, \pi[$ (see figure 11.11). This leads us to an interpretation of the local quaternionic phase.

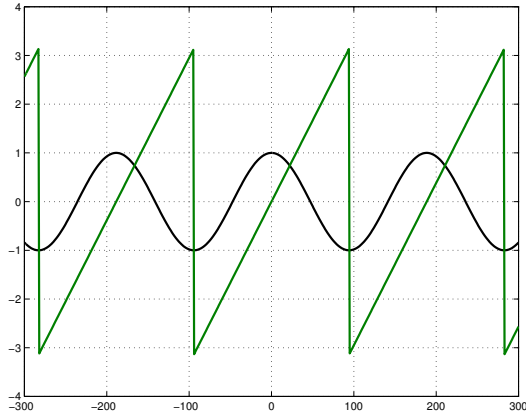


Fig. 11.11. The cosine function and its local phase

We make a similar example as in the one-dimensional case by replacing $\cos(x)$ by $\cos(x)\cos(y)$. The first two components of the local phase ϕ and θ turn out to approximate the spatial position: $\phi(\mathbf{x}) \approx x$ and $\theta(\mathbf{x}) \approx y$ for $(x, y) \in [0, 2\pi[\times [0, \pi[$. In general it turns out that these two components of the local phase are equivariant with spatial position. The reason for the interval $[0, 2\pi[\times [0, \pi[$, which follows mathematically from the definition of the angular phase of unit quaternions, can be understood from figure 11.12.

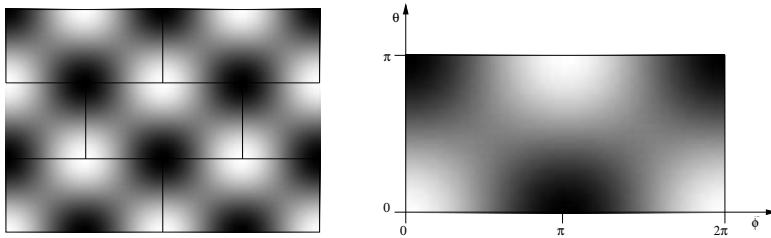


Fig. 11.12. The function $f(x, y) = \cos(x)\cos(y)$ with $(x, y) \in [0, 4\pi[\times [0, 3\pi[$ (left) and $(x, y) \in [0, 2\pi[\times [0, \pi[$ (right)

While the spatial position can be recovered uniquely from the local signal structure within the interval $[0, 2\pi[\times [0, \pi[$, there will occur ambiguities if the interval is extended. The whole function $\cos(x)\cos(y)$ can be build from patches of the size $2\pi \times \pi$. Considering this example the third component of the local phase is always zero: $\psi = 0$. The meaning of this phase component becomes obvious if we vary the structure of the test signal in the following way. The function $\cos(x)\cos(y)$ can be written as the sum

$$\cos(x)\cos(y) = \frac{1}{2}(\cos(x+y) + \cos(x-y)).$$

If we consider linear combinations of the form

$$f(\mathbf{x}) = (1 - \lambda)\cos(x+y) + \lambda\cos(x-y)$$

we find that ψ varies monotonically with the value of $\lambda \in [0, 1]$. This behavior is shown in figure 11.13.

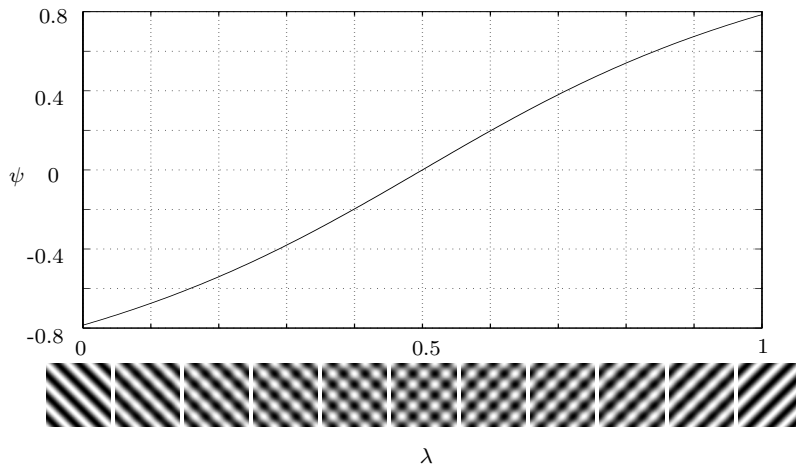


Fig. 11.13. Dependence of the third phase component ψ on the local image structure

The first two phase components, namely ϕ and θ do not change their meaning, while λ varies. Only for the values $\lambda = 0$ and $\lambda = 1$, i.e. $\psi = \mp \frac{\pi}{4}$ the structure degenerates into an intrinsically one-dimensional structure. Hence, the spatial position cannot any longer be recovered from the local structure. This corresponds to the singularity in the evaluation the angular phase of a quaternion when $\psi = \pm \frac{\pi}{4}$. In this case only $\phi \mp \theta$ can be evaluated. The remaining degree of freedom can be eliminated by setting $\theta = 0$.

11.3.4 Relations between Complex and Quaternionic Gabor Filters

There is a simple relation between complex and quaternionic Gabor filters. Each component of a complex Gabor filter with aspect ratio $\epsilon = 1$ may be written as the sum of two quaternionic Gabor filter components:

$$\begin{aligned} h_e(x, y) &= g(x, y) \cos(\omega_1 x + \omega_2 y) \\ &= g(x, y) (\cos(\omega_1 x) \cos(\omega_2 y) - \sin(\omega_1 x) \sin(\omega_2 y)) \\ &= h_{ee}^q(x, y) - h_{oo}^q(x, y) \end{aligned} \quad (11.39)$$

$$\begin{aligned} h_o(x, y) &= g(x, y) \sin(\omega_1 x + \omega_2 y) \\ &= g(x, y) (\cos(\omega_1 x) \sin(\omega_2 y) + \sin(\omega_1 x) \cos(\omega_2 y)) \\ &= h_{eo}^q(x, y) + h_{oe}^q(x, y). \end{aligned} \quad (11.40)$$

From the same quaternionic Gabor filter a second complex Gabor filter can be generated by

$$\begin{aligned} h_e(x, y) &= g(x, y) \cos(\omega_1 x - \omega_2 y) \\ &= h_{ee}^q(x, y) + h_{oo}^q(x, y) \end{aligned} \quad (11.41)$$

$$\begin{aligned} h_o(x, y) &= g(x, y) \sin(\omega_1 x - \omega_2 y) \\ &= h_{oe}^q(x, y) - h_{eo}^q(x, y). \end{aligned} \quad (11.42)$$

Thus, each quaternionic Gabor filter corresponds to *two* complex Gabor filters. Sometimes these two complex filters are denoted by h^+ (11.39, 11.40) and h^- (11.41, 11.42), respectively. The response of a signal $f(x, y)$ to a Gabor filter will be denoted by $k(x, y)$ for a complex Gabor filter and $k^q(x, y)$ for a quaternionic Gabor filter:

$$\begin{aligned} k(x, y) &= (h * f)(x, y) \\ &= ((h_e + ih_o) * f)(x, y) \\ &= k_e(x, y) + ik_o(x, y) \end{aligned} \quad (11.43)$$

$$\begin{aligned} k^q(x, y) &= (h^q * f)(x, y) \\ &= ((h_{ee}^q + ih_{oe}^q + jh_{eo}^q + kh_{oo}^q) * f)(x, y) \\ &= k_{ee}^q(x, y) + ik_{oe}^q(x, y) + jk_{eo}^q(x, y) + kk_{oo}^q(x, y). \end{aligned} \quad (11.44)$$

Theorem 11.3.1. *The filter responses of the complex Gabor filters h^+ and h^- can be obtained from k^q by*

$$k^+(x) = (k_{ee}^q - k_{oo}^q) + i(k_{oe}^q + k_{eo}^q) \quad (11.45)$$

$$k^-(x) = (k_{ee}^q + k_{oo}^q) + i(k_{oe}^q - k_{eo}^q). \quad (11.46)$$

Proof. The theorem follows from the definition of h^+ and h^- and the fact that h^q is an LSI-filter. \square

Algebraically, the relation between quaternionic and complex Gabor filters can be illuminated if we apply a mapping from the algebra \mathbb{H} to the four-

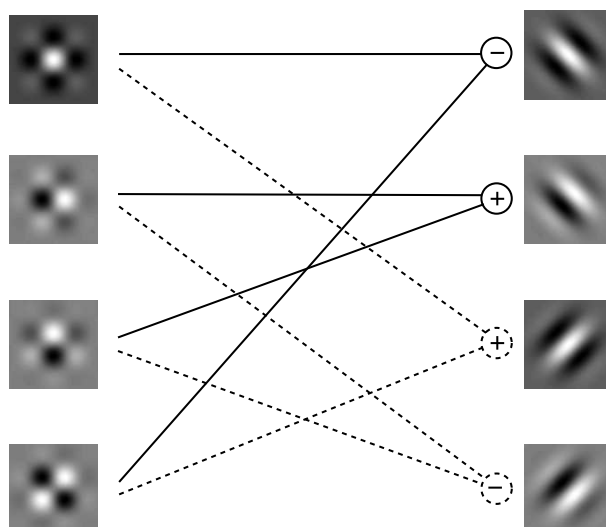


Fig. 11.14. Relation between quaternionic and complex Gabor filters

dimensional commutative hypercomplex algebra \mathcal{H}_2 introduced in chapter 9 called *switching*.

Definition 11.3.4 (Switching). *The one-to-one mapping $S_2 : \mathbb{H} \rightarrow \mathcal{H}_2$ is defined by*

$$S_2(a + bi + cj + dk) = a + bi_1 + ci_2 + di_3.$$

The multiplication table of \mathcal{H}_2 is given in table 11.3 (see also table 9.2)

Table 11.3. Multiplication table of \mathcal{H}_2

	i_1	i_2	i_3
i_1	-1	i_3	$-i_2$
i_2	i_3	-1	$-i_1$
i_3	$-i_2$	$-i_1$	1

Theorem 11.3.2. *Let h^q be a quaternionic Gabor filter. Then*

$$\eta(S_2(h^q(\mathbf{x}))) = (h^+(\mathbf{x}), h^-(\mathbf{x})) \in \mathbb{C}^2,$$

where η establishes the isomorphism between \mathcal{H}_2 and \mathbb{C}^2 :

$$\eta : \mathcal{H}_2 \rightarrow \mathbb{C}^2 \quad (11.47)$$

$$(\alpha + \beta i_1 + \gamma i_2 + \delta i_3) \mapsto ((\alpha - \delta) + i(\beta + \gamma), (\alpha + \delta) + i(\beta - \gamma)) \quad (11.48)$$

The same is true for the filter responses to real images

$$\eta(S_2(k^q(\mathbf{x}))) = (k^+(\mathbf{x}), k^-(\mathbf{x})) \in \mathbb{C}^2.$$

Proof. The theorem follows directly from applying η to $S_2(h^q(\mathbf{x}))$ and the definition of h^+ and h^- . \square

11.3.5 Algorithmic Complexity of Gabor Filtering

When performing a Gabor filtering on the computer we have to use discrete Gabor filter masks of the form: $h = [h_{m,n}]_{m,n \in \{1, \dots, M\}}$ with

$$h_{m,n} = h\left(m - \frac{M-1}{2}, n - \frac{N-1}{2}\right), \quad (11.49)$$

where the right hand side is the continuous Gabor filter as in Def. 11.3.2.

Using this convention the Gabor filter mask is an $M \times M$ matrix. The origin is located at the center of the matrix, therefore it is advantageous to choose M odd, in order to have a pixel in the center of the filter mask. The frequencies u and v count how many periods fit into the filter mask in horizontal and vertical direction, respectively.

The number of multiplications required by the convolution of an $N \times N$ image with an $M \times M$ filter mask in a direct manner is $O(N^2 M^2)$. When the filter mask h is separable ($h = h_c * h_r$), where h_c and h_r are a column vector and a row vector of length M , respectively, the filtering operation is of linear asymptotic complexity. Since the convolution operation is associative we can write the filtering as

$$F = f * (h_c * h_r) = (f * h_c) * h_r. \quad (11.50)$$

Thus, the number of required multiplications reduces to $O(N^2 M)$. It has been shown how complex Gabor filter components can be constructed as the sum of components of a quaternionic Gabor filter. Since quaternionic Gabor filters are separable, **this opens the possibility of implementing the convolution with complex Gabor filters in a separable way.** This result is especially important since Gabor filters are known to be not exactly steerable [174]. Figure 11.15 clarifies this result in "image notation".

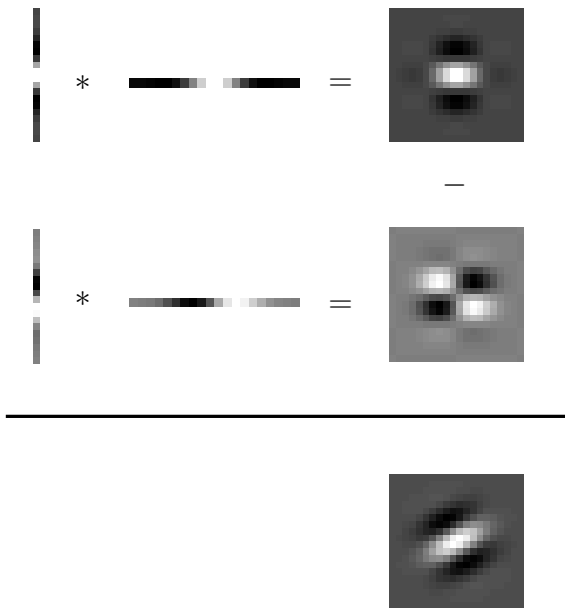


Fig. 11.15. The real part of a complex Gabor filter as linear combination of separable quaternionic Gabor filter components

11.4 Texture Segmentation Using the Quaternionic Phase

The task addressed in this section is: *Segment a given image into uniformly textured regions.* This so-called *texture segmentation* problem is one branch of the general problem of *image segmentation* which is one important step in many computer vision tasks. Regarding global variations of gray values or mean gray values over some neighborhood is in most cases not sufficient for a correct segmentation. For this reason rather the global variations of local measures characterizing the texture have to be regarded.

The posed problem is rather vague since the term *texture* is not well defined and there is no unique way of characterizing mathematically the local gray-value variations perceived as texture by human observers. For this reason very different approaches to texture segmentation have been taken. As local measure for the characterization of texture local statistical properties [103, 125] and local geometric building blocks (textons) [127] have been used among others. Another whole branch in texture segmentation research is based on the local spatial frequency for characterizing texture. On the one hand the Gabor filter based approaches to texture analysis are motivated by psychophysical research since 2-D Gabor filters have proven to be a good model for the cortical receptive field profiles [57] while on the other hand they

are supported by the observation that a whole class of textures (so-called *deterministic textures*) give rise to periodic gray value structures. We will restrict ourselves to the Gabor filter based approaches here. In the following the term texture will always be understood as *image texture* in contrast to *surface texture*. While surface texture is a property of a 3D real-world object, image texture in this context is a property of a 2-D intensity image.

In the following sections we analyze in detail the pioneering work of Bovik et al. [26] and in parallel introduce the corresponding quaternionic Gabor filter based approach to texture segmentation. In the final section we discuss our result and make some remarks on other texture segmentation approaches based on Gabor filters.

11.4.1 The Gabor Filter Approach

Bovik et al. [26] introduced a Gabor filter based approach to texture segmentation. As mentioned above, texture segmentation is the task of segmenting an image into uniformly textured regions. According to Bovik's approach a uniform texture is described by a dominant frequency and orientation. Thus, different textures occurring in a given image are supposed to differ significantly at least in either the dominant frequency or the dominant orientation.

This assumption leads to the following simple *texture model*. An image containing only one homogeneous texture is modeled as

$$\begin{aligned} f_i(\mathbf{x}) &= c_i(\mathbf{x}) \cos(2\pi(u_i x + v_i y)) + s_i(\mathbf{x}) \sin(2\pi(u_i x + v_i y)) \\ &= a_i(\mathbf{x}) \cos(2\pi(u_i x + v_i y) + p_i(\mathbf{x})), \end{aligned} \quad (11.51)$$

where the amplitude $a_i = \sqrt{c_i^2 + s_i^2}$ and the phase $p_i = -\tan^{-1}\left(\frac{s_i}{c_i}\right)$ are assumed to vary slowly, i.e. in such a way that the dominant frequency component is always well approximated by (u_i, v_i) . The characterizing dominant frequency and orientation of the texture f_i are $|\mathbf{u}_i| = \sqrt{u_i^2 + v_i^2}$ and $\alpha_i = -\tan^{-1}\left(\frac{v_i}{u_i}\right)$, respectively.

A textured image containing n different textures f_i is then given by n textures of the form (11.51) each of which occurs in exactly one connected region \mathcal{R}_i of the image. Defining the characteristic functions z_i of the regions

$$z_i(\mathbf{x}) = \begin{cases} 1 & \text{if } \mathbf{x} \in \mathcal{R}_i \\ 0 & \text{else,} \end{cases}$$

we can write the texture image f as

$$f(\mathbf{x}) = \sum_{i=1}^n f_i(\mathbf{x}) z_i(\mathbf{x}). \quad (11.52)$$

The regions \mathcal{R}_i are assumed to define a partitioning of the domain of f , i.e. $\sum_{i=1}^n z_i(\mathbf{x}) \equiv 1$ and $z_i(\mathbf{x}) z_j(\mathbf{x}) \equiv 0$ if $i \neq j$. The set of all possible

textures f will be denoted by \mathcal{T} . This texture model fits optimally the texture segmentation technique applied by Bovik et al.

The first step in the segmentation procedure is devoted to *filter selection*. In this stage the parameters of a number of Gabor filters that will be used for the segmentation are chosen. For a review of possible methods we refer to Bovik's article [26]. The image f is convolved with the set of selected Gabor filters h_i which yields n filtered images k_i , where n is the number of selected filters. The complex filtered images are transformed into the amplitude/phase-representation according to

$$m_i = |k_i|, \quad \phi = -\tan^{-1} \left(\frac{\mathcal{I}(k_i)}{\mathcal{R}(k_i)} \right). \quad (11.53)$$

The first level of segmentation is based on the comparison of the channel amplitudes. At this stage each pixel of the image is assigned to one channel. We will denote the region of pixels belonging to channel i by \mathcal{R}_i . The classification is simply based on the comparison of the amplitudes m_i at each position in the image:

$$\mathbf{x} \in \mathcal{R}_i \iff \arg \left(\max_{j \in \{1, \dots, n\}} (m_j(\mathbf{x})) \right) = i, \quad (11.54)$$

where the function \arg returns the index of m . A second segmentation step is based on phase discontinuities. In this step regions which contain the same texture but which are shifted against each other are separated.

11.4.2 Quaternionic Extension of Bovik's Approach

The extension of Bovik's approach to texture segmentation using quaternionic Gabor filters is straightforward. Before outlining the segmentation procedure in the quaternionic case we modify the texture model given above. If quaternionic Gabor filters are applied instead of complex filters the following texture model is more appropriate. A textured image is assumed to consist of homogeneously textured regions

$$f^q(\mathbf{x}) = \sum_{i=1}^n f_i^q(\mathbf{x}) z_i(\mathbf{x}), \quad (11.55)$$

where this time the homogeneous textures are of the form

$$\begin{aligned} f_i^q(\mathbf{x}) = & cc_i(\mathbf{x}) \cos(2\pi u_i x) \cos(2\pi v_i y) \\ & + sc_i(\mathbf{x}) \sin(2\pi u_i x) \cos(2\pi v_i y) \\ & + cs_i(\mathbf{x}) \cos(2\pi u_i x) \sin(2\pi v_i y) \\ & + ss_i(\mathbf{x}) \sin(2\pi u_i x) \sin(2\pi v_i y). \end{aligned}$$

Again, the functions cc_i , sc_i , cs_i and ss_i are assumed to vary slowly. The set of all possible textures f^q will be denoted by \mathcal{T}^q . Obviously, this model is most

appropriate for the use of quaternionic filters, since the four terms exactly correspond to the modulation functions of the components of a quaternionic Gabor filter. In figure 11.16 two model textures are shown which demonstrate the difference between the two models.



Fig. 11.16. Two examples of textured images. Left: A textured image fitting Bovik's texture model (11.52). Right: An image fitting the extended texture model (11.55). For simplicity, in both examples constant coefficients have been chosen

Note that the quaternionic texture model comprises Bovik's model as a special case, i.e. $\mathcal{T} \subset \mathcal{T}^q$.

The first stages of the segmentation procedure stay basically the same as described in the previous section. Only slight modifications have to be made. The filter selection stage is performed by a peak-finding algorithm in the quaternionic power spectrum. The difference is that here the peak finding is only performed over one quadrant of the frequency domain instead of one half in the complex approach. As we have shown when introducing the quaternionic analytic signal in section 11.2.3, one quadrant of the quaternionic frequency domain contains the complete information about the image.

Having selected a set of n quaternionic Gabor filters h_i^q the textured image is convolved with these filters, which yields the filtered images k_i^q . These image values are transformed into the polar representation of quaternions introduced in section 8.3.1. This leads to an amplitude/phase-representation $(m_i, \phi_i, \theta_i, \psi_i)$ of the filtered images.

Since we have shown that complex Gabor filters are contained in the quaternionic Gabor filters, the first levels of Bovik's approach, i.e. channel assignment and detecting phase discontinuities, can as well be performed using quaternionic Gabor filters. Thus, we do not go into details on these steps but show which additional information is contained in the quaternionic Gabor filter response, which can be used for segmentation purposes.

As shown in Fig. 11.13 the ψ -component of the phase holds the information about the mixture of two superimposed frequency components, i.e. f_1 and f_2 . Denoting the mixed texture by $f = (1 - \lambda)f_1 + \lambda f_2$ there is a one-

to-one mapping of ψ to λ . Thus, it is possible to use the ψ -component of the local quaternionic phase in order to separate regions belonging to the same frequency channel but having different structure according to the continuum of structures shown in Fig. 11.13.

11.4.3 Experimental Results

We demonstrate the segmentation power of the ψ -component of the local quaternionic phase first on a synthetic texture consisting of three different textures (figure 11.17). This image resembles an image used by Bovik ([26] p. 64, fig. 6), with the difference that in [26] only two different regions are used. The third region (upper right and lower left region), which is the superposition of the two orthogonally oriented sinusoidals, can not be segmented using the complex approach. In contrast, the ψ -component of the quaternionic phase distinguishes not only local frequency and orientation but also local structure as explained in the last section. See also figure 11.19 for clarification.

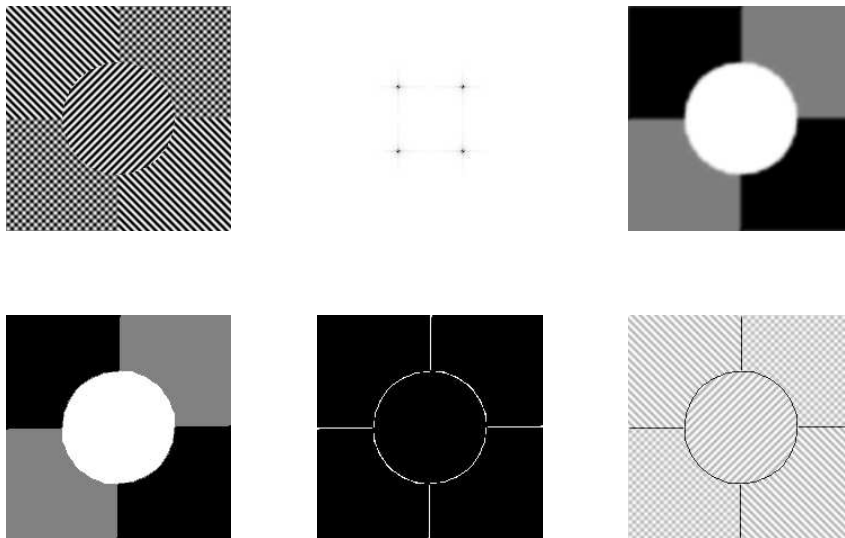


Fig. 11.17. The textured image, its QFT-magnitude spectrum, and the ψ -component of the local phase (top), and the segmentation result, the pixels which were misclassified (1.22%) and the edges of the ψ -component found by a Sobel filter superimposed to the original texture (bottom)

We tested the robustness of ψ for segmentation by adding Gaussian noise to the synthetic texture in figure 11.17. The result is shown in figure 11.18.

We added noise with zero mean and variance 1.5 and 5, respectively. The texture itself has zero mean and takes values between -1 and 1 . The SNR is -2.7 dB and -13.2 dB, respectively. Although it is almost impossible for a human observer to segment the image with the strongest noise, by means of ψ more than 78% of the pixels are correctly classified.

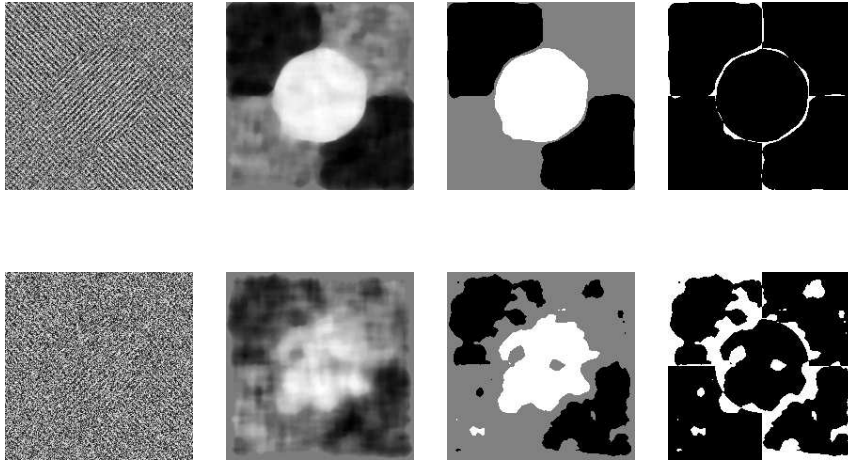


Fig. 11.18. The texture from figure 11.17 with added Gaussian noise. In the upper row the SNR is -2.7 dB, and more than 97% of the pixels are classified correctly. In the lower row the SNR is -13.2 dB and about 78% of the pixels are classified correctly. From left to right the rows show the contaminated texture, the median filtered ψ -component of the local phase, the segmented texture and the false classified pixels

11.4.4 Detection of Defects in Woven Materials

As a practical application we demonstrate how the quaternionic Gabor segmentation method can be used for the detection of defects in woven materials. We regard this task as a texture segmentation problem, where we want to segment the regular texture from defective regions. However, defects are often so small that they do not exhibit periodic structure. That makes the defect detection not feasible for a channel assignment method — complex or quaternionic — based on the magnitude of response to a certain channel filter. We test the following method here. Given a homogeneous woven texture we extract the dominant quaternionic frequency component. The image is convolved with the corresponding quaternionic Gabor filter (where the remaining parameters are chosen as $c_h = c_v = 3$) and the ψ -component of the local phase is extracted. A flaw in the texture manifests itself in a change of the lo-

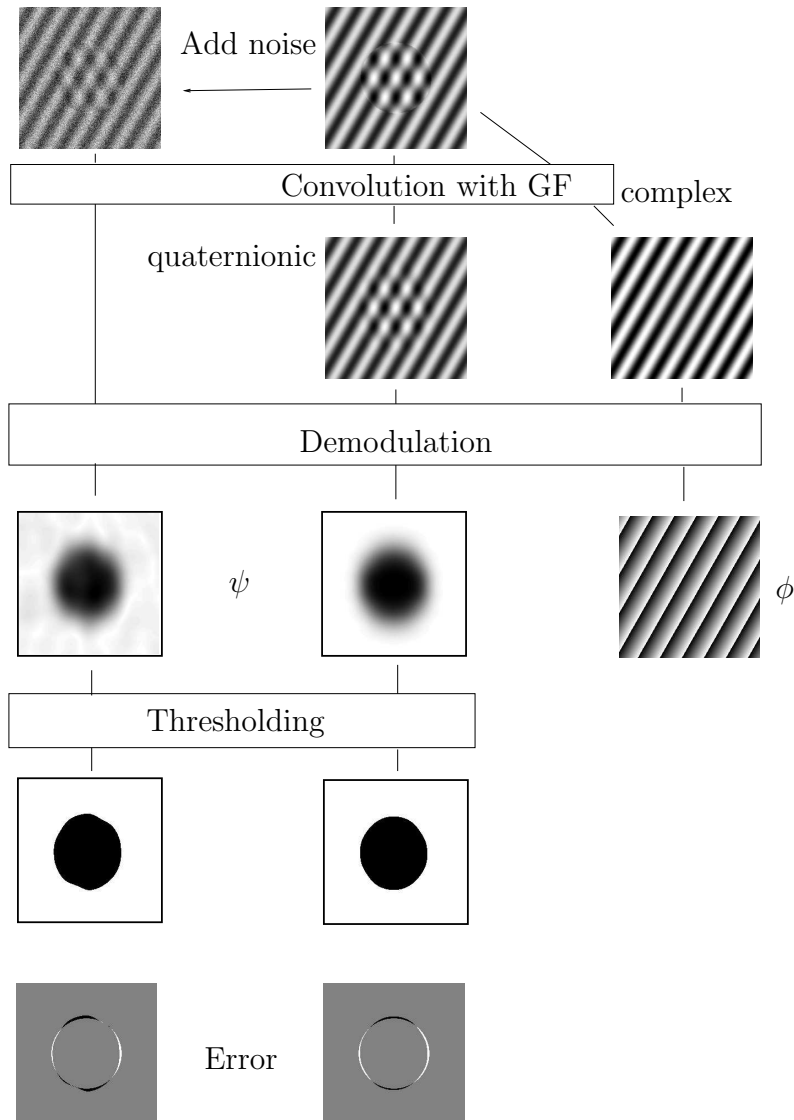


Fig. 11.19. Comparison of the complex and the quaternionic segmentation approach. The input image (top) is convolved with an optimally tuned complex (right column) and quaternionic (middle column) Gabor filter. In the second row the real parts of the filter responses are shown. The filtered images are transformed into amplitude/phase-representation. In the complex case the magnitude (not shown) is constant, and the phase ϕ is varying monotonically. No segmentation is possible. In the quaternionic case segmentation based on the ψ -component (magnitude and other phase-components are not shown) is possible. The left column is like the middle column, but with added noise (SNR=0 dB)

cal structure, which is what is measured by the ψ -phase. As the experiments show, ψ varies only very modestly within a homogeneously textured region. The mean ψ -value of a homogeneous texture f will be denoted as ψ_f . For the segmentation we chose an interval of acceptance $I_{Texture} = [\psi_f - \delta, \psi_f + \epsilon]$. The defective region will be denoted by \mathcal{R}_{Flaw} . The assignment rule is then given by

$$\mathbf{x} \in \mathcal{R}_{Flaw} \Leftrightarrow \psi(\mathbf{x}) \notin I_{Texture}.$$

As a second example we use a subregion of the texture D77 (see figure 11.20 taken from Brodatz album [32]). We apply one QGF whose central frequencies have been tuned to the main peak in the power (QFT)-spectrum of the image. In this case the frequencies are 21 cycles/image in vertical direction and 12 cycles per image in horizontal direction. In the regular part of the texture we find $\psi \approx 0.5$ while at the irregularity we get $\psi \leq 0$. Before applying a threshold, the ψ -image is smoothed with a Gaussian filter with $\sigma_{Gauss} = 1.5\sigma_{QGF}$ where $\sigma = (\sigma_1, \sigma_2)^\top$. This choice is based on an empirical result by Bovik et al. [26].

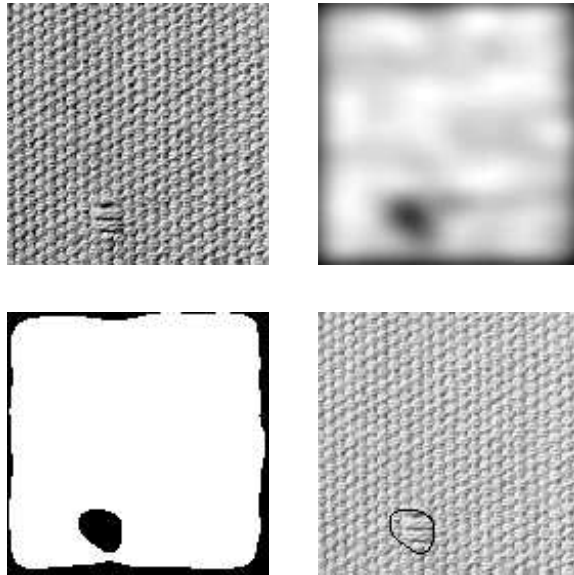


Fig. 11.20. A subregion of Brodatz texture D77 (top, left). The smoothed ψ -component of the local quaternionic phase as intensity image (top, right) and after applying a threshold (bottom, left). The edges of the thresholded ψ -phase superimposed to the input image (bottom, right)

Since at the flaw the applied filters do not match optimally, also the amplitude of the filter output yields a hint for the defect searched for. However, the amplitude is very sensitive to changing lighting conditions as shown in the following experiments. However, ψ is insensitive to changes in contrast. This is important, because of the fact that the lighting conditions are not necessarily optimal (e.g. not homogeneous) in practical applications [74].

We simulate changing lighting conditions by adding a gray-value ramp with constant slope (figure 11.21) and by changing the contrast inhomogeneously (figure 11.22). In figure 11.23 the amplitude of the filter responses are shown for the different lighting conditions. A segmentation on the basis of the amplitude envelopes is not possible by a thresholding procedure.

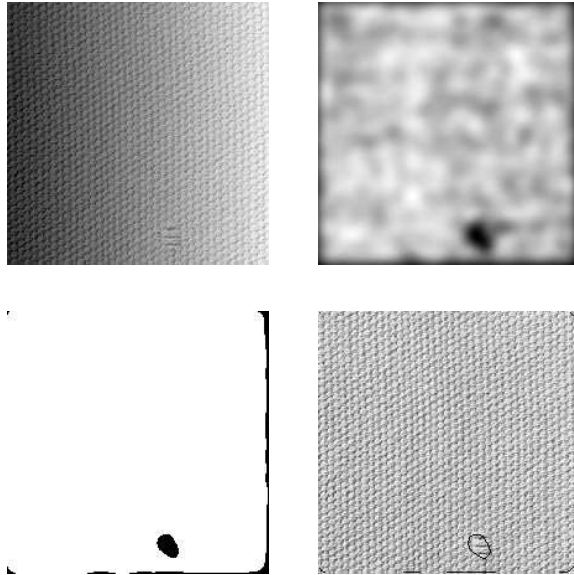


Fig. 11.21. As in figure 11.20. To the original image a gray value ramp with constant slope is added

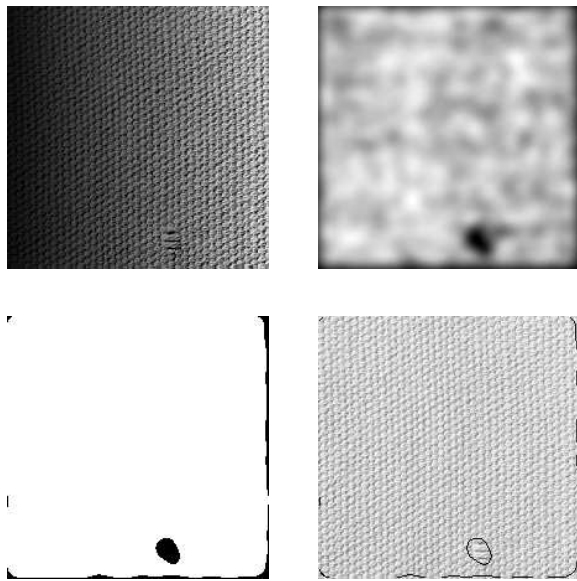


Fig. 11.22. As in figure 11.20. The contrast is modified to vary from left (low contrast) to right (high contrast)

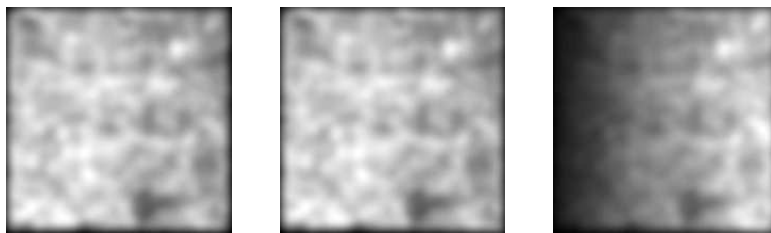


Fig. 11.23. The amplitude envelopes of the quaternionic Gabor filter response to the texture D77 under different lighting conditions. Left: Original illumination. Middle: A gray value ramp added. Right: Changing contrast

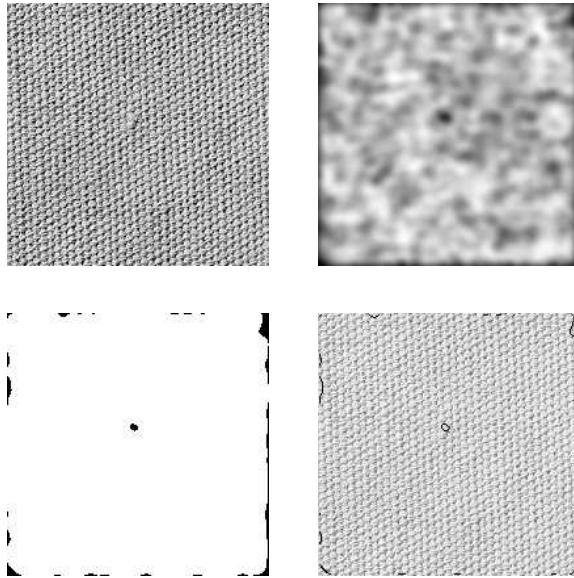


Fig. 11.24. Another subregion of D77. As in figure 11.20

The flaw detection method presented here has the advantage of being fast, since only separable convolutions have to be performed and only the ψ -component of the local phase has to be evaluated which is a pointwise nonlinear operation. The method is robust to changing lighting conditions.

11.5 Conclusion

In this chapter the quaternionic Fourier transform has been used in order to generalize the concept of the analytic signal which is well-known in 1-D signal theory to 2-D in a novel manner. Based on the quaternionic analytic signal the instantaneous quaternionic phase has been introduced. The local phase concept as introduced in this chapter is based on the approximation of an analytic signal by a Gabor filtered image. In order to introduce a local quaternionic phase, quaternionic Gabor filters have been introduced as windowed basisfunctions of the quaternionic Fourier transform. The local quaternionic phase has been used for texture segmentation where it could be shown that the ψ -component of the quaternionic phase yields a novel feature and provides useful information for the segmentation.